Pharmaceutical Research
https://doi.org/10.1007/s11095-025-03837-z

ORIGINAL RESEARCH ARTICLE

In Vitro-In Vivo Correlation Of Amorphous Solid Dispersion Enabled Itraconazole Tablets

Ana L. Coutinho[1] · Asmita Adhikari[1,2] · Samuel Krug[1] · Maureen Kane[1] · R. Gary Hollenbeck[1] · Stephen W. Hoag[1] · James E. Polli[1]

Received: 18 November 2024 / Accepted: 9 February 2025

Abstract

Purpose There are scarce reports on *in vitro-in vivo* correlation (IVIVC) model development of immediate-release (IR) formulations, and few investigations of the impacts of formulation and process of spray-dried solid dispersions (SDD)-based tablets on human pharmacokinetics (PK), despite commercial product successes. The goal of this study was to investigate the formulation and process factors that impact bioavailability enhancement of IR itraconazole SDD tablets; and to develop an FDA level A IVIVC that would predict in vivo PK performance from *in vitro* dissolution testing.

Methods A direct, differential-equation-based IVIVC model approach was employed, using an oral solution for post-dissolution disposition and Fast-, Medium-, and Slow-release tablets.

Results The IVIVC met FDA internal predictability for level A IVIVC requirements. The *in vitro* dissolution employed USP simulated intestinal fluid (phosphate buffer), adjusted pH 6.4, and tablets were triturated into particles prior to their immersion into dissolution media to mimic the attenuated disintegration difference between Medium and Slow *in vivo*. Credibility assessment of the FDA level A IVIVC model was performed, including model verification and validation considerations in light of the question of interest, the context of use, and model risk.

Conclusion To our knowledge, this is the first and only study that successfully developed an FDA level A IVIVC of an amorphous solid dispersion, which assessed the impact of grades of the same polymer, disintegrant level, and dry granulation processing on the performance of SDD tablets in humans.

Keywords amorphous · correlation · dispersion · dissolution · human · itraconazole · pharmacokinetics

Abbreviations

%PE	Percent prediction error
A_1	Drug amount in the central compartment
A_2	Drug amount in the peripheral compartment
ASD	Amorphous solid dispersion
AUC	Area under the curve
$AUC_{0\text{-inf}}$	Area under the curve from concentration at time zero to infinity
$AUC_{0\text{-last}}$	Area under the curve from concentration at time zero to last concentration
BCS	Biopharmaceutical Classification System
C_{max}	Maximum concentration in concentration vs time profile
c_s	Drug solubility
FDA	U.S. Food and Drug Administration
F_{dis}	Fraction dissolved
GCRC	General Clinical Research Center
GI	Gastrointestinal tract
GMP	Good manufacturing practices
HPMCAS	Hydroxypropyl methylcellulose acetate succinate
ITZ	Itraconazole
IVIVC	*In vitro-in vivo* correlation
k_d	Dissolution rate coefficient
k_{12}	Distribution rate constant from central to peripheral compartment
k_{21}	Distribution rate constant from peripheral to central compartment
k_{el}	Elimination rate constant

✉ James E. Polli
jpolli@rx.umaryland.edu

[1] Department of Pharmaceutical Sciences, University of Maryland School of Pharmacy, 20 Penn Street, Room 623, HSF2 Building, Baltimore, MD 21201, USA

[2] Current Affiliation: Janssen Research & Development LLC, 920 US 202, Raritan, NJ 08869, USA

Published online: 11 March 2025

k_p	Permeation rate constant
k_{pp}	Precipitation rate constant
LC–MS/MS	Liquid chromatography with tandem mass spectroscopy
LSR	Least-squared regression
M	Mass of undissolved drug as a function of time
M_0	Drug dose
M_d	Mass of dissolved drug as a function of time
MLE	Maximum likelihood estimates
NCA	Non-compartmental analysis
PBPK	Physiologically based pharmacokinetic modeling
PBBM	Physiologically based biopharmaceutics modeling
PK	Pharmacokinetics
pK_a	Acid dissociation constant
SDD	Spray-dried dispersion
S_f	Scaling factor
SIF	Simulated intestinal fluid
T_{lag}	Lag time
T_{max}	Time to maximum concentration
UPLC	Ultra performance liquid chromatography
USP	United States Pharmacopeia
V	Volume of central compartment
V_{diss}	Volume of the dissolution vessel

Introduction

Amorphous solid dispersion (ASD) is an enabling technology that can enhance oral bioavailability of poorly-water soluble drugs [1]. This study focused on an ASD, more specifically spray-dried dispersions (SDD), of itraconazole. This project involved itraconazole SDD tablet manufacturing, *in vitro* dissolution experiments, their human pharmacokinetic (PK) clinical study, and an *in vitro-in vivo* correlation (IVIVC) model.

Itraconazole is an anti-fungal drug approved in the United States as an oral capsule (Sporanox capsules) and oral solution (Sporanox oral solution) [2, 3]. It is a weak base with a pK_a of 3.7, and its solubility is pH dependent. Itraconazole solubility at pH 1.0 is approximately 4 µg/mL, and at neutral pH, its solubility drops to < 1 ng/mL [4]. Hence, itraconazole has been used as a model drug to study enabling formulations, such as ASD, to improve drug solubility.

In this study, we investigated the use of SDDs fabricated with the cellulose-based polymer hypromellose acetate succinate (HPCMAS) and itraconazole. There are three grades of HPMCAS in the market: -L, -M, and -H. These grades have different proportions of acetyl, methoxyl, and succinoyl functional groups attached to the cellulose ring [5]. The proportion of these functional groups confers different abilities of the polymer to interact with the drug and the aqueous media [6].

Previous work has shown that HPMCAS grades -L and -M provided better solubility and dissolution performance of itraconazole SDD than grade -H [7–10]. Hence, the study here employed SDD of itraconazole and HPMCAS grades -L and -M, excluding -H grade.

Although SDD is a prevalent manufacturing approach to produce an ASD, there is a knowledge gap in predicting human PK from SDD tablet dissolution. As of December 2023, three out of 55 ASD-based drug products approved by the Food and Drug Administration (FDA) submitted an IVIVC as part of their regulatory package. However, none of these IVIVC submitted were acceptable by the FDA [11].

An IVIVC is a mathematical model correlating the relationship between *in vitro* properties (i.e., drug dissolution tests) with *in vivo* performance (i.e., concentration vs time profiles). IVIVC can provide a surrogate for *in vivo* bioequivalence studies (i.e., biowaivers), specify *in vitro* dissolution acceptance parameters, and establish a link between drug product critical quality attributes and its vivo performance [12, 13]. IVIVC can directly assess the impact of the drug product characteristics, including formulation/manufacturing variations, on clinical performance [14]. Although the FDA IVIVC guidance only pertains to extended-release (ER) oral dosage forms, IVIVC of immediate-release oral formulations has been successfully performed [12, 14–23]. Notwithstanding previous literature reports on itraconazole IVIVC, none of these reports aimed at using the correlation model to understand formulation characteristics and their impact on human PK [16, 17]. To the best of our knowledge, there are no successful FDA level A IVIVC of ASD drug formulation in the literature. Therefore, an objective of this study was to devise an FDA level A IVIVC model of itraconazole SDD tablets. This objective was motivated by the desire to identify an *in vitro* dissolution method that would predict human performance, as well as to determine formulation and manufacturing parameters that impacted *in vivo* itraconazole SDD tablet performance. We aimed to find an in vitro dissolution condition that would be sensitive to *in vivo* performance differences without being overly sensitive. The two main formulation factors selected here for this IVIVC study were HPMCAS grade (grades -L versus -M) and sodium starch glycolate disintegrant level. Additional factors to promote a range of dissolution profiles, denoted Fast, Medium, and Slow, were slugging pressure and tablet compaction pressure.

Mathematical models that inform decisions about the safety, efficacy, or quality of drug products, such as FDA level A IVIVC analysis, presumably require model credibility assessment that extends beyond common academic practices. For regulatory decision-making, it has been advocated to establish that a model is credible for its intended use, and that verification and validation are important activities, although consensus of how to assess model credibility has not been achieved [24]. Three important concepts in model credibility assessment are the question of interest, the context of use, and the model risk [24–26]. In Table I, the question of interest was: Can an FDA level A IVIVC be developed for an ASD? The planned context of use for the IVIVC developed here is academic and without regulatory purpose. However, the planned IVIVC would provide insights into the impacts of HPMCAS grade type, amount of disintegrant, slugging pressure, and tablet compaction pressure on *in vivo* PK, including the ability of in vitro dissolution to predict *in vivo* PK. Therefore, elements of model credibility of the above IVIVC are discussed here.

Results here show the development of a successful FDA level A IVIVC, using a direct differential-equation-based approach. Using observed Loo-Riegelman absorption profiles (i.e., *in vivo* data) as targets for in vitro dissolution, a final dissolution testing involved pH 6.4 and individually crushed tablets to reflect *in vivo* tablet disintegration. The IVIVC employed a time scaling factor that slowed in vitro profiles to mimic *in vivo* pharmacokinetic profiles. The IVIVC model credibility was assessed in terms of verification and validation elements.

Materials and Methods

Materials

Hypromellose acetate succinate (HPMCAS, Aquasolve) grades -L and -M were sourced from Ashland (Covington, KY). Itraconazole USP grade was purchased from Letco Medical (Wayne, PA). Dichloromethane and methanol (NF grade) were obtained from Sigma-Aldrich (St. Louis, MO). Silicified microcrystalline cellulose NF and sodium starch glycolate NF were sourced from JRS Pharma (Patterson, NY). Magnesium stearate NF was obtained from Spectrum Pharmaceuticals (Henderson, NV). Purified water was from a Barnstead GenPure purification system (Thermo Scientific, Waltham, MA). HPLC-grade sodium phosphate monobasic, sodium hydroxide, hydrochloric acid, methanol, and triethylamine were acquired from Sigma-Aldrich (St. Louis, MO).

Itraconazole Tablet Formulation

Three itraconazole amorphous solid dispersion immediate-release tablets (100 mg) were developed with fast-, medium-, and slow-release rates (e.g., Fast, Medium, and Slow tablets). The development of these tablet formulations have been previously described [7–9]. Tablets were manufactured as spray-dry dispersion (SDD) with HPMCAS as the polymer carrier and 20% drug load. Tablets differed in the HPMCAS grade, amount of disintegrant (sodium starch glycolate), slugging pressure, and tablet compaction pressure. Tablet formulation and manufacturing parameters are presented in Table II. Supplemental Table S1 shows the chemical differences between HPMCAS grades -L and -M.

Tablet manufacturing was performed at the University of Maryland Good Manufacturing Practices (GMP) facility at the School of Pharmacy in Baltimore, MD. SDD intermediate material was produced using a Buchi B-290 spray dryer (New Castle, DE) in closed-loop mode (2:1 w/w solution of dichloromethane and methanol). SDD was dried overnight, mixed with silicified microcrystalline cellulose, sodium starch glycolate, and magnesium stearate, and then passed through a U.S. standard sieve #100 (150 µm). The powder blend was dry granulated by producing slugs using a Styl'One compaction simulator (Korsch AG; Berlin, Germany). The slugs were then milled by trituration until able to pass through a #100 mesh sieve. The granules (764 mg, containing 100 mg itraconazole) were then compacted using the Styl'One compaction simulator to produce tablets. Slugging and tablet compaction pressure is shown in Table II.

Table I Model Credibility Assessment Framework for Itraconazole ASD IVIVC

Question of interest	Can an FDA level A IVIVC be developed for an ASD?
Context of Use	IVIVC model is academic and without regulatory purpose
Decision Consequence	Low
Model Influence	High
Model Risk	Medium
Clinical Data Used for Validation	Human PK data from SSD fast-, medium-, and slow-release tablets
Comments	Model development used the oral solution human PK disposition. Compartmental model was used to describe observed PK data

Table II Itraconazole (ITZ) 100 mg Tablet Formulation Composition and Manufacturing Parameters. Spray-Dried Dispersion (SDD) Intermediate Contained Either HPMCAS-L or HPMCAS-M; SDD Drug Load was 20%. Tablets were Manufactured via Dry Granulation. HPMCAS Grades -L and -M Differed in the Levels of the Acetyl, Methoxyl, and Succinoyl Functional Groups

Tablet-release	Formulation	Slugging Pressure	Tablet Compaction Pressure
Fast	65.5% ITZ/HPMCAS-L SDD 30% silicified microcrystalline cellulose 4% sodium starch glycolate 0.5% magnesium stearate	40 MPa	75 MPa
Medium	65.5% ITZ/HPMCAS-M SDD 30% silicified microcrystalline cellulose 4% sodium starch glycolate 0.5% magnesium stearate	40 MPa	85 MPa
Slow	65.5% ITZ/HPMCAS-M SDD 33% silicified microcrystalline cellulose 1% sodium starch glycolate 0.5% magnesium stearate	20 MPa	100 MPa

In Vitro Dissolution

Preliminary *in vitro* dissolution was performed in USP II (paddle) dissolution apparatus (MODEL SR8PLUS, Hansen Teledyne; Chatsworth, CA) using 900 mL United States Pharmacopeia (USP) simulated intestinal fluid (SIF) pH 6.8 media without enzyme at 37°C and 100 rpm. USP SIF composition involved dissolving 6.8 g of potassium phosphate monobasic per liter (e.g., 50 mM phosphate buffer). pH was adjusted with NaOH or HCl. USP SIF does not use bile acids. The dissolution methodology was revised after the clinical study (e.g., final dissolution testing). Dissolution conditions were evaluated with varying pH, paddle rotation speed, and form of the formulation introduced in the vessel, as shown in Table S2.

Preliminary *in vitro* dissolution testing was overly sensitive to the differences in the amount of disintegrant in Medium and Slow tablets. To lower the effects of disintegrant level on dissolution profile, tablets were triturated into crushed tablets (i.e., into tablet granules). A crushed tablet was obtained by triturating an individual tablet using a ceramic mortar and pestle until all material passed through a U.S. standard sieve #14 (1400 µm). Each crushed tablet was used separately in individual dissolution vessels. The yield of each crushed tablet was greater than 96%.

For all dissolution tests, the dissolution samples (2 mL) were filtrated with a 0.45 um pore size filter, discarding the first 1 mL and collecting the second 1 mL. The filtered samples (100 µL) were diluted with 900 µL of mobile phase (75% methanol/25% buffer) for itraconazole quantification analysis [7].

Itraconazole Clinical Study

An open-label, randomized, single-dose, fasted, randomized, four-way cross-over pharmacokinetic study was conducted on 12 healthy adults. The drug products tested were Fast, Medium, and Slow tablets manufactured for this study and a commercially available oral solution (Sporanox, Janssen). An intravenous itraconazole product ceased to be marketed in the US and was not available for human use here. The dose of all drug products was 100 mg. The study was approved by the University of Maryland Institutional Review Board (NCT04035187, HP-00084585) and was performed in accordance with the ethical standards as laid down in the 1964 Declaration of Helsinki and its later amendments. The study was conducted at the General Clinical Research Center (GCRC) at the University of Maryland Medical Center in Baltimore, MD, USA. Informed consent was obtained from all participants.

Before a dosing visit, subjects fasted for 10 h before a single dose administration of an itraconazole product. Only water was allowed during fasting, and participants stopped water consumption one hr before and one hr after drug administration. The itraconazole drug product was administered with 240 mL of water. Lunch was served 4 h after dosing.

Blood was collected for PK analysis pre-dose, 1, 2, 3, 4, 5, 6, 8, 12, 15, 24, 36, and 48 h after drug administration. When participants received the oral solution, a blood draw was also collected 72 h after drug administration.

Itraconazole Quantification *In Vitro* and *In Vivo*

In vitro itraconazole quantification employed Waters ACQUITY H Class UPLC with a fluorescence detector (250/380 nm) (Milford, MA) and the methodology has been described in the literature [7]. The flow rate was 0.6 mL/min with isocratic flow of mobile phase 75% methanol and 25% buffer solution (0.1% triethylamine with pH adjusted to 3.0 with phosphoric acid). Run time was 2 min, and retention time was 0.7 min. The column used was 2.1 × 50 mm ACQUITY BEH C18 1.7 µm (Waters Corporation; Milford, MA) which was heated to 45°C. Stock solution of

itraconazole in dimethyl sulfoxide (100 µg/mL) was used to prepare standards diluted in mobile phase. A linear calibration curve ($r^2 > 0.999$) was established in the range of 0.5–12 µg/mL.

The clinical study plasma samples were analyzed by the University of Maryland School of Pharmacy Mass Spectrometry Center in Baltimore, MD using a Waters-I Class UPLC system coupled with a Waters Xevo TQ-XS mass spectrometer (Milford, MA). A detailed LC–MS/MS methodology for itraconazole quantification from plasma samples for this study has been published [27].

IVIVC Modeling

In vitro dissolution, *in vivo* PK, and IVIVC modeling were conducted using Phoenix WinNonlin/NLME (version 8.3.3, Certara, St. Louis, MO). T_{lag} was implemented via Maximum Likelihood Estimates (MLE) Object as a dosepoint function. The non-stiff option (DVERK) numerical integration method in Phoenix was used to solve the differential equations. Observed PK parameters (e.g., C_{max}, T_{max}, AUC) of the average PK profiles were calculated using non-compartmental analysis (NCA). The oral solution average PK profile was fitted to a library of compartmental models using least-square regression. The preliminary compartmental parameters were used as a starting point in the final disposition model in Phoenix NLME. The Loo-Riegelman object in Phoenix was used to deconvolve all formulations PK profiles using estimates from the initial compartmental analysis. The fraction drug absorbed profile for each tablet formulation was used to devise the target *in vitro* dissolution profile (i.e., to devise a final *in vitro* dissolution test). Dissolution models were fit to the *in vitro* dissolution data of Fast, Medium, and Slow tablets [28, 29]. The final dissolution model was chosen based on visual inspection of model fits, minimal least-residual squares, and the smallest number of parameters to be estimated.

IVIVC model development was conducted using a direct differential-equation-based approach. This was a one-stage method in which the differential equations describing the itraconazole dissolution and PK were solved directly using numerical integration. Itraconazole *in vivo* dissolution, permeation, distribution, and elimination processes were described by a set of differential equations describing drug mass transfer among the dissolution, permeation, central, and peripheral compartments. These differential equations were coded in Phoenix NLME.

The steps of model development and assessment are shown in Fig. 1. Steps followed the recommended workflow for oral biopharmaceutics-focused applications, including elements of identification of model objectives, model development and verification, model validation, and model application [30]. This physiologically based pharmacokinetic (PBPK) modeling and physiologically based biopharmaceutics modeling (PBBM) ["PBPK/PBBM"] guidance anticipates the need for model refinement. Here, as reflected in Fig. 1, two model refinement steps were 1) final *in vitro* dissolution testing that was conducted after clinical study and aimed to match absorption profiles from deconvolution, and 2) the use of a scaling factor (S_f) since tablet dissolution profiles *in vivo* were slower than *in vitro*. The FDA IVIVC guidance allows for a scaling factor [12].

Prediction Error Assessment

Following FDA IVIVC Guidance, which is referenced by the "PBPK/PBBM" guidance, each predicted PK profile should be compared to the observed PK profile for that same formulation. The percent prediction error (%PE) of the PK parameters (i.e., C_{max}, AUC) were calculated based on Eq. 1. The criteria for internal predictability of an FDA level A IVIVC is that the average absolute %PE of all formulations is 10% or less for C_{max} and AUC. In addition, the %PE of each formulation C_{max} and AUC should be 15% or less [12].

$$\%PE = \left[\left(\frac{Observed\ value - Predicted\ value}{Observed\ value}\right)100\right] \quad (1)$$

Sensitivity Analysis and Dissolution Specifications

A sensitivity analysis was conducted to assess the sensitivity of predicted *in vivo* tablet PK against *in vitro* dissolution profile. Dissolution profiles were varied by modifying drug solubility (c_s) parameter value in a stepwise fashion to define a dissolution safe space and dissolution specification that would impact C_{max} or $AUC_{0\text{-last}}$ by at most ± 20%.

Results and Discussion

Itraconazole Tablet Manufacturing

As expected from prior studies under identical spray drying manufacturing, itraconazole in SDD intermediate was amorphous, as determined from differential scanning calorimetry [7–9]. Tablets used in the clinical study passed pre-specified criteria of slugging compaction pressure, tablet compaction pressure, and tablet weight. Tablet stability testing was conducted after manufacturing and involved 28-day stability at room temperature and under the International Council for Harmonisation of Technical Requirements for Pharmaceuticals for Human Use (ICH) accelerated conditions (40 C, 75% relative humidity), and at the end of clinical study. Tablets were found to be within specification (data not shown).

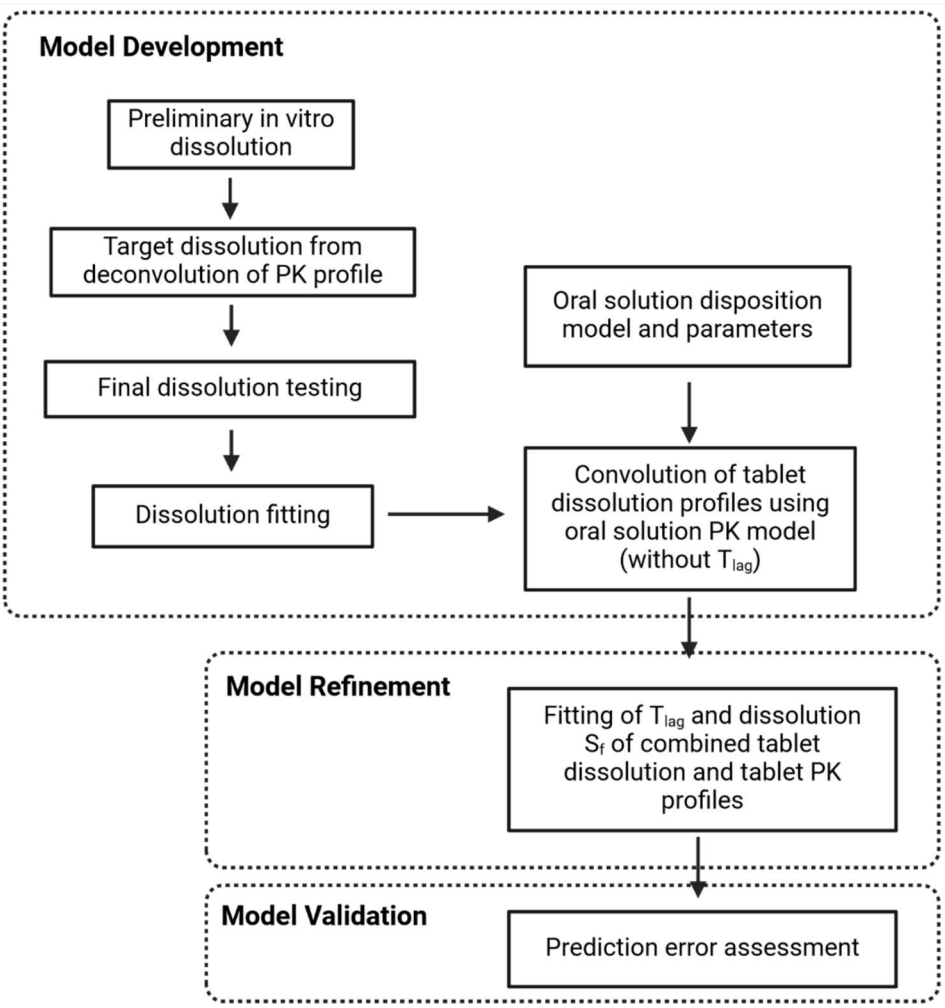

Fig. 1 IVIVC model development and assessment steps. Clinical PK study evaluated Fast, Medium, and Slow formulations, and an oral solution. The disposition model was obtained from the oral solution PK profile. Oral solution two-compartment PK parameters were applied in the convolution of tablet dissolution profiles without lag time (T_{lag}). It was apparent that tablet PK profiles exhibited a Tlag *in vivo*. It was also apparent that tablet dissolution profiles *in vivo* were slower than *in vitro*, such that a scaling factor (S_f) was required. Hence, an IVIVC model was fitted to allow for a tablet T_{lag} and S_f. Prediction error assessment followed the FDA IVIVC Guidance. Preliminary dissolution testing was conducted before clinical study. Final dissolution was conducted after clinical study and aimed to match absorption profiles from deconvolution.

In Vivo Clinical Study

As planned, twelve subjects completed the study (e.g., completed four PK rounds). Their demographic information is shown in Table S3. Eight adverse events occurred, but all of them were mild and expected based on itraconazole package insert and resolved within 48 h of onset. No serious adverse events occurred. More details on the clinical study analysis and results can be found in the Supplemental Material (e.g. Fig. S1).

Table III shows formulation PK parameters from non-compartmental analysis (NCA), both for each the

Table III Formulation PK Parameters from Non-Compartmental Analysis (NCA). Top Table Lists PK Parameters of the Average Profile Which is the Focus of this IVIVC Analysis. Bottom Table Lists Mean PK Parameters of 11 Individual Profiles. All Analysis Excluded Subject-002

PK parameters of average PK profile

Formulation	C_{max} (ng/mL)	T_{max} (h)	$AUC_{0\text{-}last}$ (ng*h/mL)	$AUC_{0\text{-}inf}$ (ng*h/mL)
Oral solution	254.6	1	1614.6	1751.4
Fast tablet	148.6	2	1304.6	1520.5
Medium tablet	91.6	3	988.9	1205.3
Slow tablet	81.8	3	837.4	982.0

Average PK parameters of individual profiles

Formulation	C_{max} (ng/mL)	T_{max} (h)	$AUC_{0\text{-}last}$ (ng*h/mL)	$AUC_{0\text{-}inf}$ (ng*h/mL)
Oral solution	268.4	1.3	1605.1	1790.0
Fast tablet	178.8	2.6	1299.3	1532.4
Medium tablet	106.0	3.4	985.6	1181.6
Slow tablet	103.1	3.5	875.2	1051.7

average profile and the mean of n = 11 individual profiles. The average profile is the focus of this IVIVC analysis. For each C_{max} and AUC, rank order was: Oral solution > Fast > Medium > Slow, a nontrivial result. Figure 2 also illustrates this rank order. Additionally, there was a rank order agreement where C_{max} and AUC mean parameters across individual subjects were examined. Geometric mean ratios for Fast versus Medium were 1.67, 1.38, and 1.35 for C_{max}, $AUC_{0\text{-last}}$, and $AUC_{0\text{-inf}}$, respectively. Geometric mean ratios for Slow versus Medium were 0.87, 0.90, and 0.90 for C_{max}, $AUC_{0\text{-last}}$, and $AUC_{0\text{-inf}}$, respectively. There were meaningful differences across the four formulations, resulting in meaningful differences across their PK profiles.

Absolute and Relative Bioavailability of Test Formulations

A strength of this IVIVC design was the availability of itraconazole intravenous (IV) and oral solution PK data from Heykants *et al*. (1989) [31]. Table III shows $AUC_{0\text{-inf}}$, and absolute and relative bioavailabilities from Heykants *et al*. AUC of IV and oral solution were 4600 and 1920 ng*h/mL, respectively. The oral solution bioavailability was reported to be 41.7%. Table III also shows $AUC_{0\text{-inf}}$ of tested formulations here. $AUC_{0\text{-inf}}$ of oral solution, Fast, Medium, and Slow were 1751.4, 1520.5, 1205.3, and 982.0 ng*h/mL, respectively. Hence, using the IV $AUC_{0\text{-inf}}$ from Heykants *et al*., the absolute bioavailabilities of tested formulations here were 38.1, 33.0, 26.2, and 21.3%, respectively. There was good agreement in bioavailabilities of oral solution between Heykants *et al*. and here (i.e., 41.7% and 38.1%). This supports the use of Heykants *et al*. IV $AUC_{0\text{-inf}}$ to calculate the absolute bioavailability of test formulations. The relative bioavailabilities of Fast, Medium, and Slow tablets in relation to the oral solution tested here were 86.7, 68.9, and 56.0%.

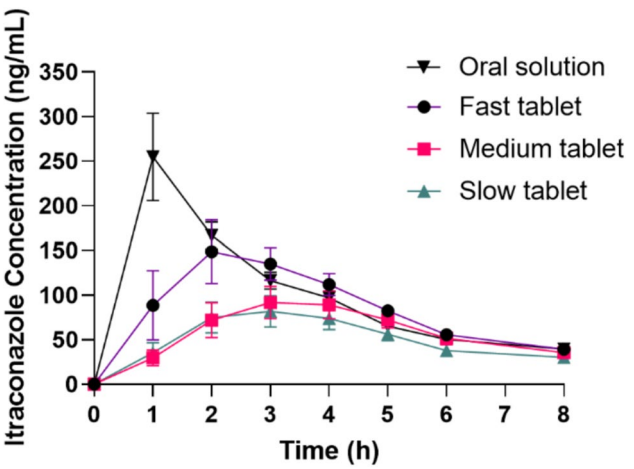

Fig. 2 Average PK profiles of itraconazole oral solution, Fast, Medium, and Slow tablets. Profiles differed from one another and their rank order reflected formulation design.

Oral Solution Disposition Model and Parameters

Initial PK compartmental analysis using least-square regression was conducted on oral solution profile to identify a compartmental model from 1-, 2-, and 3-compartment models, with and without a lag time. Results indicated, per the lowest Akaike information criterion (AIC) value, that the best fit was a 2-compartment model without a lag time. These compartment parameters were used as initial estimates in the subsequent analysis that involved differential equations in the Maximum likelihood estimates (MLE) Object. First-pass metabolism was not qualitatively considered. Itraconazole first-pass metabolism has been reported to be 44% based on IV formulation hepatic clearance and liver blood flow [31]. Here, we estimate the oral absolute bioavailability of Sporanox oral solution to be 38.1% (i.e., 38.1 mg was systemic available of the 100 mg dose administered here); this estimate of 38.1% used AUC observed here from Sporanox oral solution and AUC from IV formulation from Heykants *et al*. (1989) [31].

The PK parameters estimated by the 2-compartment disposition model using MLE Object were permeation rate constant (k_p) of 19.4/h, distribution rate constant from central to peripheral compartment (k_{12}) of 0.221/h, distribution rate constant from peripheral to central compartments (k_{21}) of 0.0807/h, elimination rate constant (k_{el}) of 0.201/h, and volume of distribution (V) in the central compartment of 102 L. Observed and predicted profiles are shown in Figure S2.

The permeation rate constant (k_p) of 19.4/h reflects very rapid itraconazole intestinal permeability, where the permeability of the dissolved drug is distinct from drug dissolution. Assuming a ratio of intestinal luminal area versus intestinal volume (i.e., A/V ratio) of 11/cm, k = 19.4/h (or 0.00539/sec) implicates an apparent itraconazole intestinal permeability of $490*10^{-6}$ cm/sec [32]. Again, this perspective reflects very rapid itraconazole intestinal permeability [32, 33].

Deconvolution of PK profile to Devise Target Dissolution

The average PK profiles were deconvolved using the Loo-Riegelman method in Phoenix. The Loo-Riegelman method was chosen because the PK profile for all formulations followed a 2-compartment model. Deconvolution yielded a fraction absorbed profile that was corrected for relative bioavailability to the oral solution, as shown in Fig. 3. The relative bioavailabilities of Fast, Medium, and Slow tablets were 86.7, 68.9, and 56.0%, respectively (Table IV). These absorption profiles were used to estimate the extent of the

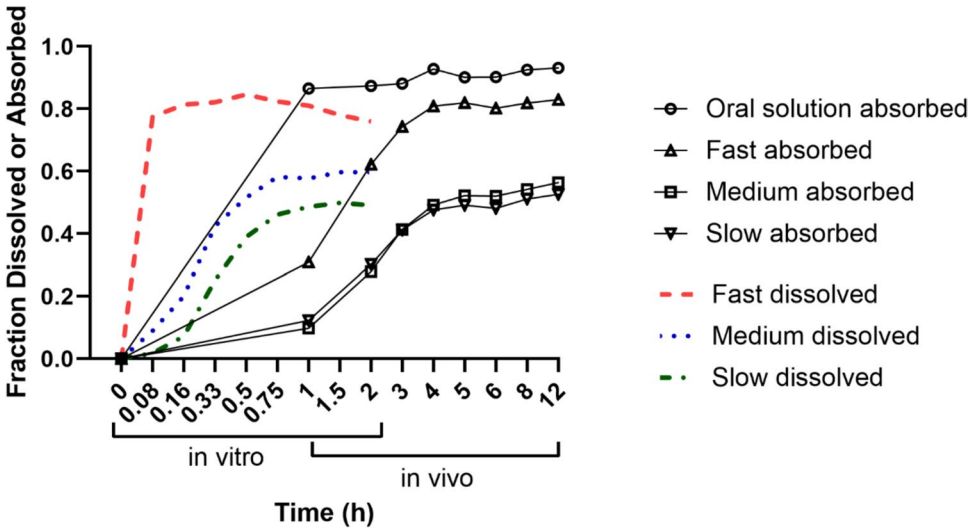

Fig. 3 Plot of final dissolution profiles of Fast, Medium, and Slow tablets and their corresponding Loo-Riegelman absorption profiles. Extent of *in vitro* dissolution and extent of *in vivo* absorption were similar for each formulation. However, *in vitro* dissolution was faster than *in vivo* absorption, as highlighted by "*in vitro*" and "*in vivo*" being added to X-axis. X-axis not drawn to scale.

Table IV Absolute and Relative Bioavailability of Itraconazole Formulations from Literature and Measured here. All Formulations were 100 mg and Tested in Healthy Volunteers in the Fasted State. The Absolute Bioavailability was Calculated relative to the IV Formulation from Heykants *et al*. (1989) [31]. Relative Bioavailability was Calculated Relative to the Study's Own Oral Solution (i.e., Heykants et al. or Oral Solution here). The $AUC_{0\text{-inf}}$ of Formulations Here Used the Average PK Profile Without Subject-002 and Calculated using NCA. Oral Solution Here Exhibited an Absolute Bioavailability of 38.1%

Heykants et al. 1989 Study[73]	$AUC_{0\text{-inf}}$ (ng*h/mL)	Absolute bioavailability (%)	Relative bioavailability (%)
IV	4600	100	——
Oral solution	1920	41.7	100
Capsule	720	15.7	37.5
US FDA Package Insert[51]	$AUC_{0\text{-inf}}$ (ng*h/mL)	Absolute bioavailability (%)	Relative bioavailability (%)
Sporanox capsule	722	15.7	—-
Formulations here	$AUC_{0\text{-inf}}$ (ng*h/mL)	Absolute bioavailability (%)	Relative bioavailability (%)
Oral solution	1751.4	38.1	100
Fast	1520.5	33.0	86.7
Medium	1205.3	26.2	68.9
Slow	982.0	21.3	56.0

drug dissolution *in vivo*, given that the oral solution showed 38.1% bioavailability. These Loo-Riegelman profiles became the targets for the final *in vitro* dissolution testing, including the extent of dissolution.

In Vitro Dissolution Test Conditions

The preliminary dissolution method employed USP apparatus II, 100 rpm, 900 mL, USP SIF pH 6.8 [7, 9]. It was inspired by the compendial method of itraconazole capsules (i.e., SGF without enzyme, as itraconazole is more soluble at low pH than neutral pH) but where pH was necessarily increased to pH 6.8 to allow for HPMCAS dissolution [34]. HPMCAS is an enteric polymer [5]. Itraconazole tablets using HPMCAS essentially did not dissolve at all at pH 1.2, as expected (data not shown). In Fig. S3, Fast tablets exhibited the fastest dissolution rate and highest drug release extent, followed by Medium tablets. Fast and Medium tablets reached maximum drug release at around 20 min. Slow tablets showed the slowest dissolution rate and took 240 min to reach maximum drug release, in part due to its especially slow *in vitro* disintegration.

The preliminary dissolution profiles in Fig. S3 failed to predict the Medium and Slow tablet performance *in vivo* (data now shown, although evident by inspection), where Medium and Slow PK profiles were different, but not vastly different. A final in vitro dissolution test was needed that was less sensitive to *in vitro* disintegration than the preliminary *in vitro* dissolution testing. Many experimental conditions were evaluated by modifying dissolution media pH, paddle rotation speed, and formulation form (i.e., whole and crushed tablets) to try to mimic Loo-Riegelman profiles,

particularly in their relative extents of 86.1%, 67.1%, and 55.7% versus oral solution. Table S2 lists all dissolution conditions evaluated.

Media pH conditions ranged between 6.0 and 6.8. The disintegration of the enteric polymers HPMCAS-L and -M grades is pH dependent, with -L grade disintegrating at pH 5.8 and -M grade at pH 6.0. HPMCAS-M grade is more resistant to disintegration relative to -L grade in this pH range.

The *in vivo* results showed that *in vivo* disintegration differences between Medium and Slow were less remarkable than in preliminary *in vitro* dissolution testing, which was very overly sensitive to disintegrant level, and slugging and compaction pressures. There were substantial composition and dry granulation process differences between Medium and Slow tablets, which each employed HPMCAS-M grade. Relative to Medium, Slow employed less disintegrant, resulting in a slower disintegrating tablet (Table II). This large *in vitro* disintegration difference also reflected work-hardening phenomena, as Slow tablets employed lower slugging pressure and higher compaction pressure [9, 35]. However, *in vivo*, these differences – while still remarkable – were attenuated compared to the preliminary *in vitro* differences. To lower the effects of disintegrant level on *in vitro* dissolution profile, particularly for Slow, tablets were triturated into crushed tablets.

The dissolution profiles of Fast whole and crushed tablets are shown in Figure S4. Dissolution for this formulation was not sensitive to tested media pH changes, as expected, nor to formulation form (i.e., whole vs crushed tablet). Regardless of the formulation form, the Fast formulation dissolved rapidly within 5 min and reached maximum fraction dissolved by 10 min. A decrease in drug dissolution shortly after maximum dissolution was reached indicated a small degree of precipitation *in vitro*.

The dissolution profiles of Medium whole and crushed are shown in Figure S5. Dissolution for this formulation was sensitive to media pH, as expected. A decrease in pH led to a decrease in the dissolution rate and extent of the Medium formulation. Among whole tablets, the fastest dissolution rate and highest dissolution extent was observed at pH 6.8, followed by tablets at pH 6.6, 6.5, 6.4, 6.3, and 6.2. No dissolution was observed at pH 6.0. At pH 6.4, there were no differences between whole and crushed Medium tablets in the dissolution rate or extent.

The dissolution profiles of Slow whole and crushed tablets are shown in Figure S6. Like Medium whole tablets, the dissolution rate and extent of Slow whole tablets decreased when pH decreased from 6.8 to 6.5, as expected. Slow tablets possessed the same grade of HPCMAS as Medium tablets (i.e., -M grade), but had four times less sodium starch glycolate. This difference, along with processing conditions, contributed to very slow intact Slow tablet disintegration during *in vitro* dissolution compared to intact Medium tablets.

Dissolution profiles of Slow crushed tablets were investigated in order to increase the Slow dissolution rate and extent, reflecting Slow greater *in vivo* similarity to Medium than predicted by preliminary *in vitro* dissolution (data not shown). Importantly, Slow crushed tablet showed a faster rate of dissolution than whole tablets at pH 6.5 and pH 6.8, and a higher extent of dissolution than whole tablets at pH 6.5. By triturating the Slow tablet, the *in vitro* dissolution matched the target profile provided by the *in vivo* fraction absorbed profile.

Based on the results from PK deconvolution, final dissolution target profiles were elucidated. As shown in Fig. 3, the terminal *in vivo* fractions absorbed were 86.1, 67.1, and 55.7% for Fast, Medium, and Slow, compared to oral solution. The dissolution test that yielded the closest dissolution rate and extent to Loo-Riegelman profiles that are normalized for relative bioavailability to the oral solution employed crushed tablets and USP apparatus II (paddle) with 50 rpm and phosphate buffer pH 6.4 as media at 37°C. This dissolution test condition yielded a maximum percent dissolved of 84.7, 59.7, and 49.8% for Fast, Medium, and Slow formulations, respectively (Fig. 3).

In Vitro Dissolution Modeling

Final dissolution profiles for the IVIVC model are shown in Fig. 4 (panel A). Several dissolution models were fitted, including Weibull, which provided closest fits, but with more fitted parameters. The Polli model was selected for the IVIVC model since it provided acceptable fit and only one parameter (i.e., k_d) was fitted. It was expected that a dissolution time-scaling factor would be needed, such that the Polli model, where only k_d was fitted, was viewed as favorable [29].

For all three tablet formulations, the change in fraction undissolved was described by Eq. 2, where M is the mass of drug undissolved, and Dose was the mass of drug available to be absorbed at $t=0$ (i.e., 38.1 mg, see discussion below), V_{diss} is the dissolution vessel volume, k_d is the dissolution rate coefficient, and t is time. c_s was taken as the highest drug concentration from the dissolution model [i.e., 0.0358 mg/mL (84.7% dissolved), 0.0253 mg/mL (59.7% dissolved), and 0.0211 mg/mL (49.8% dissolved) for Fast, Medium, and Slow, respectively]. k_d was the single parameter fitted. Units of k_d are identical to the units of the z-factor dissolution model, although they have a slightly different interpretation than that of z-factor [29]. This dissolution equation considered non-sink condition effects (i.e., bulk drug concentration is $<33\%$ of c_s, leading to a decrease in dissolution) and incomplete drug solubility and dissolution.

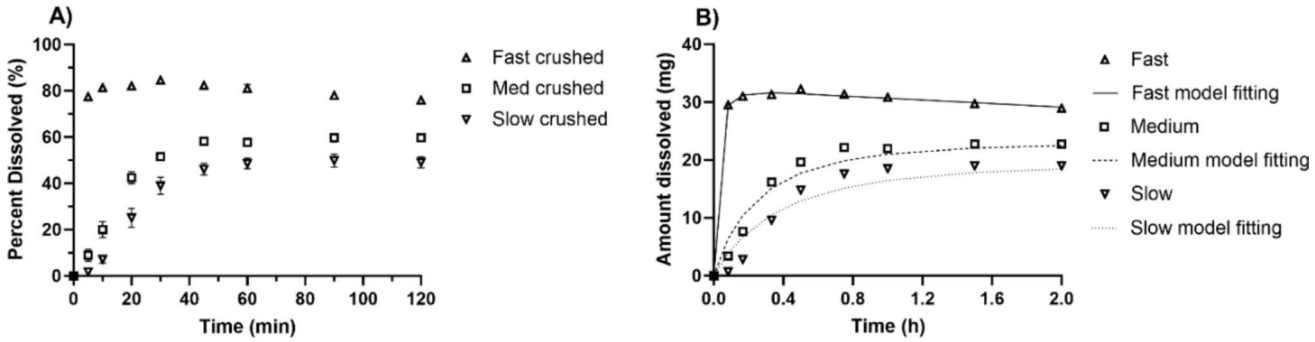

Fig. 4 Final itraconazole dissolution profiles of Fast, Medium, and Slow tablets. Panel (**A**) shows dissolution profiles from crushed tablets using USP apparatus II, SIF pH 6.4, and 50 rpm. Panel (**B**) shows the corresponding amount of drug dissolved profile based on the oral solution exhibiting an absolute bioavailability of 38.1%. Hence, 38.1 mg in Panel B is equal to 100% dissolved in Panel (**A**).

$$\frac{dM}{dt} = -k_d M\left(c_s - \frac{Dose - M}{V_{diss}}\right) \tag{2}$$

The change in dissolved drug was described by Eq. 3 for Fast (with precipitation) or Eq. 4 for Medium and Slow (without precipitation). In Fig. 4, the Fast formulation showed a slight decrease in drug dissolved *in vitro* over time. Hence, precipitation was added to Fast dissolution modeling. In Eq. 3 and Eq. 4, M_d was the mass of drug dissolved and k_{pp} was the precipitation rate constant for Fast. The observed drug precipitation from Fast here was anticipated, given the prior observed precipitation from L-grade SDD and not M-grade SDD [10].

$$\frac{dM_d}{dt} = k_d M\left(c_s - \frac{Dose - M}{V_{diss}}\right) - k_{pp}\left(\frac{M_d}{V_{diss}}\right) \tag{3}$$

$$\frac{dM_d}{dt} = k_d M\left(c_s - \frac{Dose - M}{V_{diss}}\right) \tag{4}$$

Itraconazole *in vitro* dissolution profiles are shown in Fig. 4 (Panel A). Dissolution was assumed to be the rate-limiting step in itraconazole absorption and systemic availability. Since the oral solution does not require a dissolution step for drug absorption, the absolute bioavailability of the oral solution represented the maximum amount of drug that reached the systemic circulation after absorption and first-pass metabolism. The absolute bioavailability of the oral solution here relative to IV formulation in the literature was 38.1%, in agreement with Heykants *et al*. (Table IV). Hence, the maximum amount of itraconazole that could be dissolved *in vivo*, and hence be absorbed and systemic bioavailable *in vivo*, was set to 38.1 mg (i.e., 100% drug dissolved denoted 38.1 mg dissolved). Again, first-pass metabolism was not qualitatively considered.

Based upon *in vitro* percent dissolved profile in Fig. 4 Panel A, the mass of drug dissolved profile was calculated and plotted in Fig. 4 Panel B. Equation 2 and Eq. 3 were fitted to the dissolution profile of the Fast formulation; and Eq. 2 and Eq. 4 were fitted to the dissolution profile of the Medium and Slow formulations. The applied c_s values, fitted k_d values, and fitted k_{pp} are listed in Table V.

From small volume studies, the kinetic solubility of itraconazole from HMPCAS SDD in pH 6.8 was observed to be about 0.08 mg/mL for L grade and about 0.06 mg/mL for M-grade [10]. These independent observations are supportive of the dissolution model approach.

Table V Dissolution Parameters for Fast, Medium, and Slow Itraconazole Tablets. Dissolution Rate Coefficient (k_d), Drug Solubility (c_s), and Precipitation Rate Coefficient (k_{pp} for Fast tablet) were Fitted to Dissolution Data [Amount of Drug Dissolved (mg) Versus Time] (Fig. 4 Panel B). Fitted Scaling Factor (fitted S_f) was Obtained Separately for Each Formulation, Where Fast used Eq. 8 and Eq. 9, While Each Medium and Slow used Eq. 8 and Eq. 10. Regression Scaling Factor (Regression S_f) was Obtained by Regression Fitted S_f vs k_d Across All Three Formulations. Scaling Factors were Less Than Unity and Served to Slow Dissolution *In Vivo* Relative to *In Vitro* Dissolution. NA Denotes Not Applicable (i.e., No Drug Precipitation)

	k_d (mL/mg per h)	c_s (mg/mL)	k_{pp} (mL/mg per h)	Fitted S_f (unitless)	Regression S_f (unitless)
Fast	1807 ± 143	0.0358	45.49 ± 3.63	0.0191	0.0178
Medium	103.6 ± 12.5	0.0253	NA	0.151	0.213
Slow	68.67 ± 10.65	0.0211	NA	0.277	0.217

Convolution of Tablet Dissolution Profiles Without T_{lag}

The drug mass in the central compartment (A_1) and peripheral compartments (A_2) were described by Eq. 5 and Eq. 6, respectively. k_{21} is the distribution rate constant from the peripheral to the central compartment, k_{12} is the distribution rate constant from the central to the peripheral compartment, and k_{el} is the elimination rate constant.

$$\frac{dA_1}{dt} = M_d k_p + A_2 k_{21} - A_1 k_{12} - A_1 k_{el} \quad (5)$$

$$\frac{dA_2}{dt} = A_1 k_{12} - A_2 k_{21} \quad (6)$$

$$C = \frac{A_1}{V} \quad (7)$$

Equation 7 was used to calculate the drug concentrations from drug mass where V is volume of distribution of the central compartment. Parameter values k_p, k_{12}, k_{21}, k_{el}, and V were obtained from the oral solution fit as described above. No T_{lag} was used, as the oral solution did not require one.

The predicted concentrations were then analyzed by visual examination, NCA and predictive error analysis. Although the total drug exposure of the predicted PK curve was within the acceptable criteria, C_{max} was overpredicted for all formulations (data not shown). This overprediction was readily evident from the relative fast *in vitro* dissolution compared to the slower Loo-Riegelman profiles (Fig. 3). Additionally, as expected, a short T_{lag} for tablets appeared appropriate (data not shown). Therefore, a dissolution scaling factor and a T_{lag} were pursued.

Addition of Lag Time and Scaling Factor to the IVIVC

The final IVIVC model with dissolution, central, and peripheral compartments is presented graphically in Fig. 5. The disposition parameters values for k_p, k_{12}, k_{21}, k_{el}, and V from the oral solution are listed above. Values for k_d and c_s are listed above and were used in the differential equations to estimate for lag time (T_{lag}) and Scaling Factor (S_f) for each formulation.

T_{lag} was estimated to be 0.635, 0.737, and 0.656 h for Fast, Medium, and Slow formulations. The average T_{lag} of 0.676 h was subsequently used for the final IVIVC. This need for a T_{lag} for tablets, but not the oral solution, was expected, since tablets were large (i.e. 763.4 mg weight) and mostly composed of HPMCAS, an enteric polymer that does not dissolve in the stomach. Stomach empty was first needed for tablet dissolution and subsequent drug intestinal permeation.

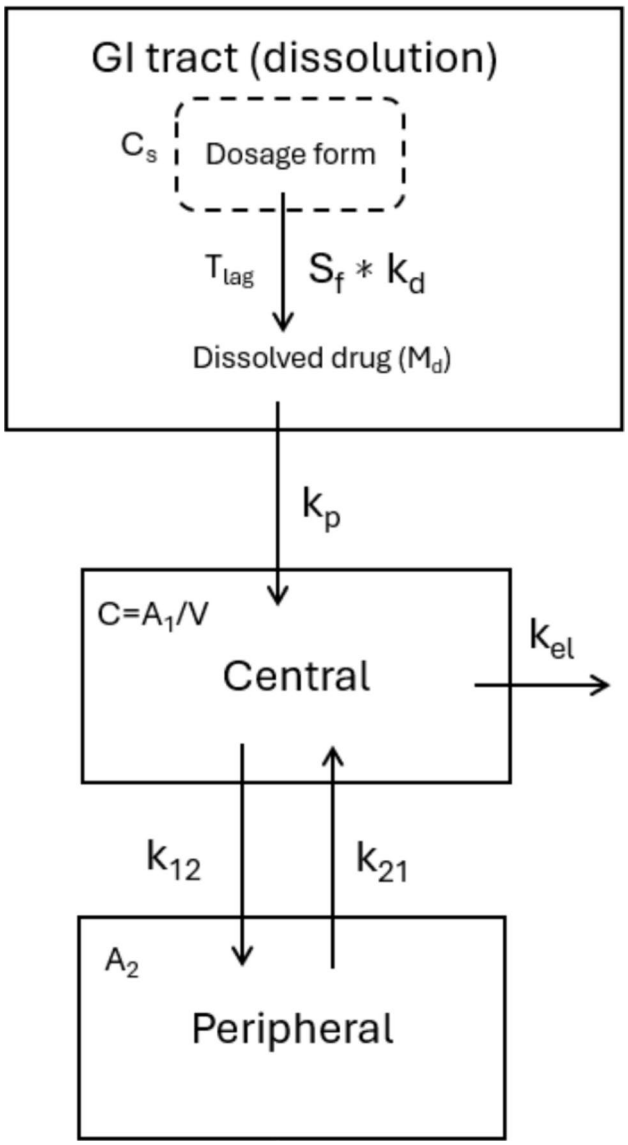

Fig. 5 Diagram representing itraconazole dissolution modeling combined with PK two-compartmental model. All kinetic processes (e.g. dissolution, permeation) are delayed until T_{lag} passes. Drug dissolution from the dosage form is mediated by the dissolution rate coefficient (k_d) in the GI tract, and drug permeation (i.e., permeation rate constant k_p) to the central compartment. Drug distribution between the central and peripheral compartments is mediated by rate constants k_{12} and k_{21}. Drug elimination is characterized by elimination rate constant k_{el}.

Here, the dissolution time-scaling factor modulated (i.e., reduced or slowed) the k_d value. S_f was fitted using the dissolution differential equations shown in Eq. 8 and Eq. 9 for the Fast formulation, and Eq. 8 and Eq. 10 for the Medium and Slow formulations. Equation 5, Eq. 6, and Eq. 7 were used to describe the *in vivo* disposition.

$$\frac{dM}{dt} = -S_f k_d M\left(c_s - \frac{Dose - M}{V_{diss}}\right) \quad (8)$$

$$\frac{dM_d}{dt} = S_f k_d M\left(c_s - \frac{Dose - M}{V_{diss}}\right) - k_{pp}\left(\frac{M_d}{V_{diss}}\right) \quad (9)$$

$$\frac{dM_d}{dt} = S_f k_d M\left(c_s - \frac{Dose - M}{V_{diss}}\right) \quad (10)$$

A linear regression analysis of the fitted S_f values versus k_d across the three formulations was performed. The resulting equation and fit are shown in Eq. 11 and Figure S7. Units of k_d in Eq. 11 were mL/mg per h, like for the z-factor dissolution model [29]. Equation 11 was used to calculate the final S_f value for each formulation, reflecting a single algorithm for *in vitro* dissolution scaling. The final S_f values were components of the final IVIVC used to predict PK profiles of each formulation as shown in Table V. S_f is unitless and it is a multiplier with a value less than 1 that slows *in vivo* dissolution relative to *in vitro* dissolution, which was more rapid than *in vivo* dissolution (Fig. 3).

$$S_f = -0.000121 \bullet k_d + 0.2251 \quad (11)$$

Overall, each aspect of the IVIVC model (i.e., dissolution component and the post-dissolution drug disposition component) entailed a small number of assumptions and parameters and exhibited favorable model parameter identifiability.

Evaluation of Internal Predictability

Internal predictability was carried out for Fast, Medium, and Slow as described in the FDA IVIVC guidance [12]. Predicted PK profiles for Fast, Medium, and Slow tablets using the IVIVC model equations (i.e., Eq. 5 through Eq. 10). T_{lag} was 0.676 h.

The results of the internal predictability analysis are shown in Table VI and Fig. 6. Each formulation C_{max}, $AUC_{0\text{-last}}$, and $AUC_{0\text{-inf}}$ showed %PE of less than 15%. Also, the average absolute %PE across all formulations for C_{max}, $AUC_{0\text{-last}}$, and $AUC_{0\text{-inf}}$ was less than 10%. Therefore, the IVIVC model successfully predicted the PK profiles of Fast, Medium, and Slow itraconazole tablets from *in vitro* dissolution. Except for T_{lag} and S_f, no IVIVC model parameter was derived from tablet PK profiles, but rather obtained from the oral solution PK profile.

Sensitivity Analysis and Dissolution Specifications

Although this IVIVC analysis is not part of a marketing authorization application, sensitivity analysis of the IVIVC was pursued here as part of an effort to assess model validity. Sensitivity analysis was conducted through identifying dissolution safe space. In particular, sensitivity analysis was conducted to assess the sensitivity of predicted *in vivo* tablet PK against *in vitro* dissolution profile. Dissolution profiles were varied by modifying dissolution c_s parameter in a stepwise fashion to define a dissolution safe space and dissolution specification that would impact C_{max} or $AUC_{0\text{-inf}}$ by ± 20%.

Table VI Percentage Prediction Error (%PE) for Fast, Medium, and Slow itraconazole Tablets. Predictions from the IVIVC Model are Compared to the Observed PK Profiles. %PE of Each Formulation C_{max} and AUC was Less than 15%. The Average Absolute PE for C_{max}, $AUC_{0\text{-last}}$, and $AUC_{0\text{-inf}}$ were 6.3, 3.4, and 5.5% and were Less than 10%

Formulation	Parameter	Observed	Predicted	%PE
Fast	C_{max} (ng/mL)	148.6	147.6	0.7
	$AUC_{0\text{-last}}$ (ng*h/mL)	1303.9	1388.1	−6.5
	$AUC_{0\text{-inf}}$ (ng*h/mL)	1518.8	1585.0	−4.4
Medium	C_{max} (ng/mL)	91.6	98.7	−7.8
	$AUC_{0\text{-last}}$ (ng*h/mL)	987.8	979.6	0.8
	$AUC_{0\text{-inf}}$ (ng*h/mL)	1205.7	1119.6	7.1
Slow	C_{max} (ng/mL)	81.8	73.4	10.3
	$AUC_{0\text{-last}}$ (ng*h/mL)	836.7	813.2	2.8
	$AUC_{0\text{-inf}}$ (ng*h/mL)	980.6	931.9	5.0

Dissolution safe space and predicted PK profiles are shown in Fig. 7. Panel A illustrates upper and lower dissolution boundaries that yield ± 20% change in C_{max} or $AUC_{0\text{-inf}}$ compared to Medium observed PK profile (i.e., that yielded at most an absolute 20% differences in either C_{max} or $AUC_{0\text{-inf}}$). Panel B illustrates the resulting PK profiles from the upper and lower dissolution boundaries. For upper dissolution boundary, C_{max} was more sensitive than $AUC_{0\text{-inf}}$ and determined the upper dissolution limit. For lower dissolution boundary, $AUC_{0\text{-inf}}$ was more sensitive than C_{max} and determined the lower dissolution limit. The target dissolution profile at 30, 60, and 90 min was 51.6, 57.7, and 59.7%, respectively. The lower bounds were 41.0, 48.3, and 50.5% at 30, 60, and 90 min, respectively. The upper bounds were 51.8, 61.6, and 65.1% at 30, 60, and 90 min, respectively.

Sensitivity analysis reflects functioning of the IVIVC model where faster dissolution results in higher C_{max} and higher exposure, and while slower dissolution results in lower C_{max} and lower exposure. This model sensitivity of C_{max} and AUC to dissolution also reflects the underlying observed *in vivo* data, supporting model validity. The performance of the IVIVC model also reflects what is generally known about oral itraconazole formulations including incomplete absorption of the oral solution and further incomplete absorption of solid dosage forms [31].

Critical Formulation Characteristics and Their Impact on In Vivo Performance

There is a poor understanding of *in vivo* ASD dissolution, such that there is a poor understanding of the relation of *in vitro* ASD dissolution to *in vivo* ASD dissolution. Compared

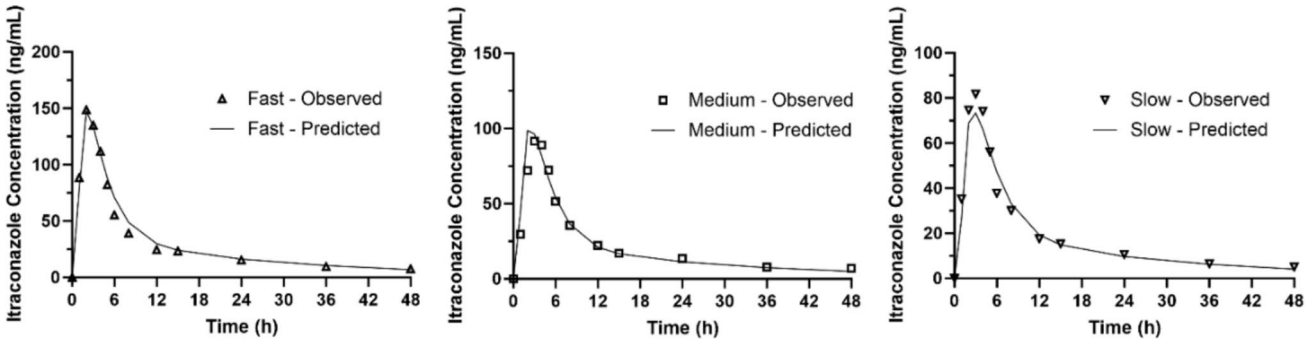

Fig. 6 Observed and predicted plasma concentration versus time profiles for Fast, Medium, and Slow tablets. %PE of each formulation Cmax and AUC was less than 15%. The average absolute PE for C_{max}, $AUC_{0\text{-last}}$, and $AUC_{0\text{-inf}}$ was 6.3, 3.4, and 5.5%.

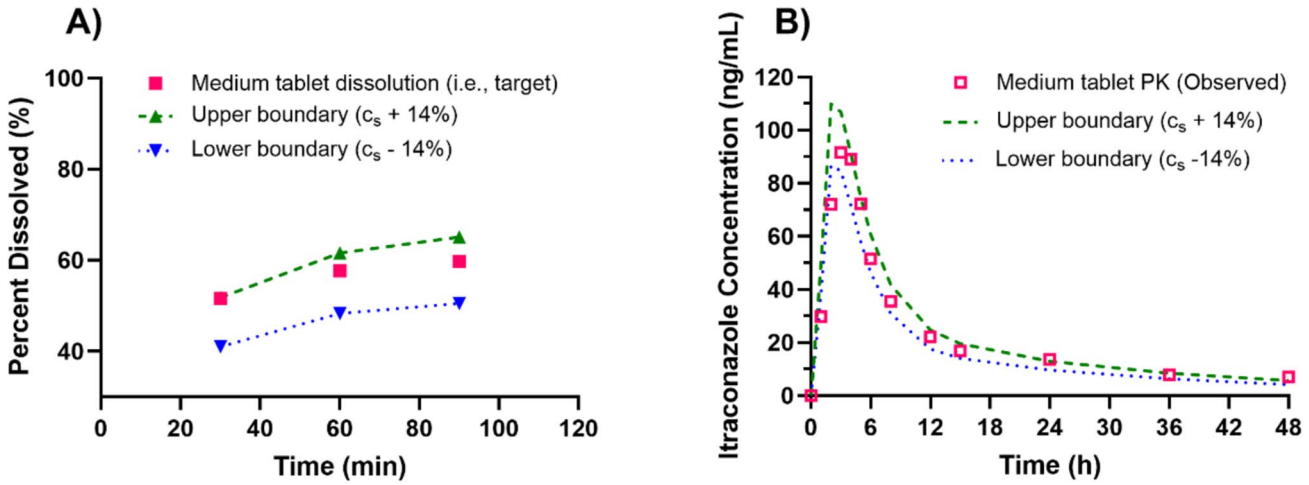

Fig. 7 Dissolution safe space and predicted PK profiles, with Medium as a target. Panel (**A**) illustrates upper and lower dissolution boundaries that yield ± 20% change (maximum) in C_{max} or $AUC_{0\text{-last}}$ compared to Medium observed PK profile; observed Medium dissolution also plotted. Panel (**B**) illustrates the resulting PK profiles from the upper and lower dissolution boundaries; observed Medium PK profile also plotted. Upper and lower boundaries identified via increasing/decreasing c_s dissolution parameter value by 14% (i.e., by 1.14-fold).

to *in vivo* ASD dissolution, there is a better understanding of *in vitro* ASD dissolution, such as itraconazole release from HPMCAS ASD involving liquid–liquid phase separation [36], although even *in vitro* ASD dissolution via the formation of drug-rich colloids is very incompletely understood [36–38]. *In vitro* dissolution methods for ASD are not standardized. Given the resulting colloids from ASD release, there is debate about how to define "dissolved drug" from ASD and even how to carry out dissolution sample analysis (e.g., filtration, centrifugation, microdialysis) [39]. The final dissolution method here, which involved filtration of sample and subsequent HPLC analysis of drug, as is commonly performed for ASD, has potential to overestimate molecularly dissolved drug by included colloid-associated drug. Presumably, *in vivo*, only molecularly dissolved drug permeated the intestinal membrane. However, it has also been proposed that colloid-associated drug is important in providing a shuttling effect across the aqueous boundary layer to promote intestinal drug absorption from ASD [36, 40–42].

A relative weakness, and future research opportunity, was the need for a dissolution time-scaling factor, although such model factors are allowed and anticipated [12, 43, 44]. Given these complexities, the need for only a single scaling factor here, with no other parameter fits associated with the test formulation PK profiles except T_{lag}, is a strength. The IVIVC model here has the potential to elucidate a better understanding of *in vivo* ASD performance.

Results indicate that HPMCAS grade was the largest contributor to differences in drug release rate, drug release extent, and PK profiles. HPMCAS-L provided a faster and higher extent of dissolution to itraconazole tablets, as well as higher *in vivo* C_{max} and AUC than HPMCAS-M based tablets. The HPMCAS-L grade also provided a higher absolute bioavailability (i.e., 33%) than the Medium (i.e., 26.2%) and Slow (i.e., 21.3%) formulations which employed HPMCAS-M grade. Fast, Medium, and Slow tablets showed greater bioavailability than the commercially available Sporanox capsules (Table 4).

The succinoyl group in HPMCAS has a pK_a of 5.0 and it is at least 50% ionized at pH > 5. The succinoyl group is responsible for the HPMCAS high solubility at intestinal pH (i.e., pH 6.0 – 7.5) when the succinoyl group is ionized. HPMCAS is increasingly un-ionized at lower pHs, and hence insoluble at gastric pH (i.e., pH ~ 1.2) [6]. In Table S1, -L grade has a higher content of succinoyl function group than -M grade (i.e., 14–18% vs 10–14%, respectively).

Previous research has shown that HPMCAS-L films and SDD outperformed those composed of HPMCAS-M in *in vitro* itraconazole dissolution and dissolution/permeation flux [7–10]. Hydrophobic acetyl and methoxyl groups of HPMCAS interact with insoluble drug to form nanostructures. Hydrophilic ionized succinoyl groups have a negative charge that stabilize drug-polymer nanostructures by interacting with aqueous solution and avoiding the formation of large hydrophobic aggregates [6]. This greater hydrophilicity of the -L grade is a contributing reason for the faster and higher drug dissolution rate and extent observed with the Fast itraconazole tablets.

Previously, HPMCAS-L grade provided greater *in vitro* dissolution of itraconazole, but greater precipitation too, compared to -M and -H grades [10]. Precipitation from -L grade was substantial in small volume dissolution under non-sink conditions [10], although precipitation was minimal but measurable here using a non-compendial USP II apparatus approach (Fig. 4). Shah and Taylor observed similar *in vitro* results for HPMCAS grades for posaconazole, using small volume dissolution under non-sink conditions [37]. Overall, -L grade provided greater *in vivo* C_{max} and AUC than -M grade, such that itraconazole *in vivo* precipitation from -L grade was potentially overestimated *in vitro*.

The need for a time-scaling factor was not a primary concern in devising a final dissolution test, where extent of dissolution and the relative rates of Medium and Slow were prioritized. Nevertheless, a reduced buffer capacity was an unexplored parameter that likely would decrease the size of this time-scaling factor. The final dissolution media utilized 50 mM phosphate buffer (pH = 6.4). Bapat *et al*. examined the impact of buffer on HPMCAS-M dissolution [45]. The interfacial pH of a dissolving HPMCAS-M compact was lower when phosphate buffer (pH = 6.5) was 20 mM than 50 mM, where buffer capacity of the 20 mM and 50 mM buffers were 8.7 and 23.8 mM/ΔpH, respectively. At 5 min, the interfacial pH dropped from pH 6.5 to about pH 5 and to about pH 6 for the 20 mM and 50 mM phosphate buffers, respectively. The lower interfacial pH reflected the lower buffer capacity of the 20 mM (versus 50 mM) phosphate buffer and was associated with a two-fold lower polymer release rate of this enteric polymer. HPMAS-M exhibits greater dissolution above pH 6 than below pH 6 [5]. The fasted upper small intestine exhibits a pH of about 6.5 and buffer capacity of about 10 mM/ΔpH [46].

As a part of *in vitro* dissolution, tablets here were triturated into crushed tablets to reflect their *in vivo* disposition. Studies have previously concluded that *in vivo* forces on dosage forms were much higher than those *in vitro* (e.g., much higher than from USP apparatus II). Kamba *et al*. have noted that agitation intensity and mechanical stress each impact dissolution and devised a ''Destructive force Dependent Release System'' to measure the mechanical destructive forces of the gastrointestinal (GI) tract [47]. Vardakou *et al*. compared dissolution data from each USP II and a Dynamic Gastric Model [48]. They concluded that the Dynamic Gastric Model could mimic *in vivo* gastric processing forces. However, USP II apparatus failed to produce any breaking forces, even though it provided high turbulent flow from the paddle at 100 rpm. Interestingly, Shameem *et al*. focused on not gastric but colonic mechanical destructive forces [49]. They concluded that such destructive forces impact tablet erosion and release from controlled-release products. Garbacz *et al*. devised a dissolution stress test device to improve the predictive ability of dissolution testing, via the mimicking of physical conditions in the gastrointestinal passage of modified release products [50]. A description of the low agitation of USP II apparatus would be incomplete without noting that some formulations can result in cone formation at the bottom of the vessel, slowing dissolution, which is not representative of *in vivo* [51].

Regulatory Considerations

We understand that grinding individual tablets prior to their introduction into the vessels is not a compendial method. It is well appreciated that the uncertainty of global regulatory acceptance of non-compendial methods has slowed the development of such alternative – and potentially better – methods [39]. This situation is problematic, as it significantly inhibits the development of dissolution methods. Even for products with limited novelty, the exclusion of non-compendial methods often results in reduced utility of dissolution testing. Traditional quality control (QC) dissolution methods generally do not provide FDA level A utility [13, 39]. For this reason, it has been considered to have a QC method for batch release and a second, biopredictive/biorelevant method for biowaiver or bridging scenarios, where the biopredictive/biorelevant method would likely involve a non-compendial element [39]. Hence, final *in vitro* dissolution testing here employed the conversion of each individual whole tablet into a crushed tablet, reflecting the *in vivo* disposition of a tablet (i.e., tablet trituration) undergoing *in vivo* dissolution.

This general goal for *in vitro* dissolution to anticipate *in vivo* performance must also consider that many products are not like itraconazole tablets here, but have low biopharmaceutic risk [52, 53]. For example, a range of formulations of

metoprolol tartrate immediate-release tablets were bioequivalent, reflecting that metoprolol dissolution from the formulations was not the rate-limiting step [28]. Any expectation that an FDA level A IVIVC analysis must require differences in extent of absorption across formulations should also consider that drugs and formulations with low biopharmaceutic risk may inherently guard against differences in extent of absorption, and in fact may be preferable products to products with higher biopharmaceutic risk, in terms of relying on *in vitro* dissolution to assess potential *in vivo* product failure.

Model Credibility Assessment

Discussed below are model verification and model validation considerations, supporting sufficient model credibility and that an FDA level A IVIVC was achieved here for an itraconazole ASD tablet formulation. In the Credibility Assessment Framework in Model-Informed Drug Development, the credibility (e.g., trust) of computational models is assessed for a particular context of use. Three concepts in the Model Credibility Assessment are the question of interest, the context of use, and the model risk (Table I) [24–26]. This IVIVC analysis does not concern any direct regulatory decision-making, but rather involves an academic study to elucidate ASD formulations and process factors. A general academic view of the purpose of modeling is to summarize data (e.g., parameterize elimination in terms of a k_{el} value) and to differentiate between competing models (e.g., 1-compartment versus 2-compartment models) [54]. Model risk assessment considers model influence and decision consequence [24]. Independently, each model influence and decision consequence may be low, medium, or high. By definition of an FDA level A IVIVC, the model would provide substantial evidence to the answer of the question of interest, such that model influence was high. Meanwhile, since an incorrect decision would not cause adverse safety or efficacy outcomes, decision consequence was low. Hence, the IVIVC model developed here was medium risk (i.e., level 3).

Given the success of this IVIVC, we envision these formulations to contribute to future research to better understand *in vivo* and *in vitro* performance of ASD, as the current *in vivo* and *in vitro* understanding of ASD product performance is poor. The question of interest was "Can an FDA level A IVIVC be achieved for an ASD?". Despite commercial successes and several approved ASD products, no FDA level A IVIVC for any ASD has been developed, although a level C IVIVC has been developed [11, 14]. IVIVC "success" is taken to include elements of the FDA IVIVC guidance, including the definition of an FDA level A IVIVC [12]. Major elements of this guidance include methods requirements (e.g., three different formulations, human testing, single dissolution method) and predictability analysis involving AUC and C_{max}. IVIVC analysis is not a mandatory regulatory requirement, and is infrequently performed and, when conducted, often unsuccessful [13]. It would even seem that the high likelihood of failure to attain IVIVC predictability hinders the appeal to even attempt an IVIVC analysis, which involves the manufacture of "batch variants" (e.g., fast and slow formulations) and their pharmacokinetic study in humans. It is unfortunate that the prospect of IVIVC failure hinders product understanding.

Verification here concerns PK software code and calculations (i.e., that the model accurately represented the underlying mathematical model) [24]. Modeling, including numerical integration, was conducted using Phoenix WinNonlin/NLME, a commercial software with decades of use across a wide community of pharmaceutical scientists. Modeling was run on a computer supported by the University of Maryland Baltimore. The underlying mathematical model is represented in Fig. 5 and defined in Eqs. 5–11. These model expressions required coding into WinNonlin/NLME (i.e., coding into WinNonlin/NLME command files). Two separate scientists inspected code (i.e., command files) for errors, relative to the underlying mathematical model. Additionally, the individual who wrote the original WinNonlin/NLME software was also consulted about code. By inspection of the above underlying mathematical model, we believe the underlying mathematical model did not require large lines of code, and that the underlying model differential equations were not prone to numerical integration instability problems. Intermediate calculations were performed to confirm code accuracy.

Validation here concerns the accuracy of the model to predict observed data and assess the correctness of model assumptions. Model validation concerning data requirements and AUC and C_{max} predictability is described in the FDA IVIVC guidance [12].

The identification of the pharmacokinetic model form benefited from the inclusion here of an oral solution in a four-way cross-over PK study design. An intravenous formulation was not available for clinical testing here. Two-compartment disposition parameters from the oral solution formulation exhibited favorable identifiability and were similar to previously reported values [31, 55]. A potential biopharmaceutic limitation of the use of Sporanox oral solution to elucidate such drug disposition here after drug release from test ASD tablets is that Sporanox oral solution is formulated with hydroxypropyl-β-cyclodextrin to solubilize itraconazole, which was absent from the test tablets here [2]. Via its complexation with drug, cyclodextrin can impact the availability of itraconazole to permeate across an absorptive membrane [56]. Nevertheless, the oral solution was included in the clinical design to identify itraconazole disposition after drug dissolution from test tablets.

The need for only a single scaling factor, and no other parameter fits associated with the test formulation PK profiles except T_{lag}, is a strength. To the extent that model overparameterization is a potential concern, the model was not

over-parameterized. A single algorithm for the scaling factor was applied across all tablet formulations.

Conclusions

An FDA level A IVIVC was successfully developed and validated for an oral itraconazole SDD. To our knowledge, this is the first study that successfully developed an FDA level A IVIVC of an ASD, which are complex in their drug release and drug absorption mechanisms (e.g., LLPS and possible "shuttling effect"). Also, previous literature studies on the development of an itraconazole IVIVC have not provided insight into specific formulations factors that affected *in vivo* performance [16, 17].

A key variable was HPMCAS grade, where -L grade provided faster and greater dissolution than -M grade (i.e., Fast tablet more than each Medium and Slow tablets). HPMCAS, as an amphiphilic polymer, allows for drugs to interact with its hydrophobic regions but also allows for hydrophilic interactions with the aqueous media. This balance of hydrophobic and hydrophilic regions in the polymer structure provides stability to the HPMCAS nanostructures that maintain the drug in the supersaturated state in the aqueous media [6].

Final *in vitro* dissolution test development was guided by observed deconvoluted pharmacokinetic profiles, including the absolute bioavailability of the oral solution. Fast, Medium, and Slow tablets showed greater bioavailability than the commercially available Sporanox capsules.

IVIVC modeling employed a direct, differential-equation-based approach. The fasted clinical study included an oral solution, allowing a post-dissolution disposition model, which was a 2-compartment model, to be constructed without relying on Fast, Medium, and/or Slow PK data. In the IVIVC model, a time-scaling factor was needed to slow *in vitro* dissolution, in terms of model *in vivo* dissolution. The need for only a single scaling factor (i.e., a time-scaling factor), and no other parameter fits associated with the test tablet formulation PK profiles except T_{lag}, was a strength. IVIVC model credibility was assessed in terms of model verification and validation. Overall, the developed FDA level A IVIVC provided linkage of *in vitro* observations about ASD formulation variables and *in vivo* performance.

Supplementary Information The online version contains supplementary material available at https://doi.org/10.1007/s11095-025-03837-z.

Acknowledgements We thank Daniel Weiner for helpful discussions about model encoding in WinNonlin/NLME software. We thank Jeffrey Fink and the nursing staff at the General Clinical Research Center (GCRC) at the University of Maryland Medical Center in Baltimore, MD, USA for their help in conducting the clinical study.

Funding This work was funded by the generosity of Marilyn Shangraw. J.E.P. is the Ralph F. Shangraw Endowed Professor in Industrial Pharmacy and Pharmaceutics. We acknowledge the support of the University of Maryland Baltimore Institute for Clinical & Translational Research (ICTR) and the National Center for Advancing Translational Sciences (NCATS) Clinical Translational Science Award (CTSA) grant numbers 1UL1TR003098 and TL1TR003100. A.L.C. NIH TL1 Clinical Research Training Award was founded by the National Center for Advancing Translational Sciences (NCATS), a component of the National Institutes of Health (NIH). Additional support was provided by the University of Maryland School of Pharmacy Mass Spectrometry Center (SOP1841-IQB2014).

Declarations

Conflict of Interest The authors have no relevant conflict of interest to disclose.

References

1. Brouwers J, Brewster ME, Augustijns P. Supersaturating Drug Delivery Systems: The Answer to Solubility-Limited Oral Bioavailability? Journal of Pharmaceutical Sciences. 2009;98:2549–72. Available from: https://linkinghub.elsevier.com/retrieve/pii/S0022354916330271. Accessed 1 Nov 2024.
2. Sporanox (Itraconazole) Oral Solution Package Insert - Janssen - U.S. Food and Drug Administration. Available from: https://www.accessdata.fda.gov/drugsatfda_docs/label/2011/020657s025lbl.pdf. Accessed 1 Nov 202.
3. Sporanox (Itraconazole) Capsules Package Insert - Janssen - U.S. Food and Drug Administration. Available from: https://www.accessdata.fda.gov/drugsatfda_docs/label/2009/020083s040s041s044lbl.pdf.. Accessed 1 Nov 202.
4. Peeters J, Neeskens P, Tollenaere JP, Van Remoortere P, Brewster ME. Characterization of the interaction of 2-hydroxypropyl-β-cyclodextrin with itraconazole at pH 2, 4, and 7. J Pharm Sci. 2002;91:1414–22. Available from: https://linkinghub.elsevier.com/retrieve/pii/S0022354916310103. Accessed 1 Nov 2024.
5. Ashland Product Grades Available: AquaSolvehypromellose acetate succinate (HPMCAS). Ashland; Available from: https://www.ashland.com/file_source/Ashland/Industries/Pharmaceutical/Links/PC-11608.12_Pharma_Product_Grades.pdf. Accessed 1 Nov 2024.
6. Friesen DT, Shanker R, Crew M, Smithey DT, Curatolo WJ, Nightingale JAS. Hydroxypropyl Methylcellulose Acetate Succinate-Based Spray-Dried Dispersions: An Overview. Mol Pharmaceutics. 2008;5:1003–19. https://doi.org/10.1021/mp8000793.

7. Honick M, Sarpal K, Alayoubi A, Zidan A, Hoag SW, Hollenbeck RG, et al. Utility of Films to Anticipate Effect of Drug Load and Polymer on Dissolution Performance from Tablets of Amorphous Itraconazole Spray-Dried Dispersions. AAPS PharmSciTech. 2019;20:331. https://doi.org/10.1208/s12249-019-1541-6.
8. Honick M, Das S, Hoag SW, Muller FX, Alayoubi A, Feng X, et al. The effects of spray drying, HPMCAS grade, and compression speed on the compaction properties of itraconazole-HPMCAS spray dried dispersions. European Journal of Pharmaceutical Sciences. 2020;155:105556. Available from: https://linkinghub.elsevier.com/retrieve/pii/S0928098720303444. Accessed 1 Nov 2024.
9. Honick M. Itraconazole-HPMCAS amorphous spray dried dispersions: composition and process factors impacting performance. [Baltimore, MD]: University of Maryland, Baltimore; 2019. Available from: http://hdl.handle.net/10713/11698.
10 Adhikari A, Polli JE. Characterization of Grades of HPMCAS Spray Dried Dispersions of Itraconazole Based on Supersaturation Kinetics and Molecular Interactions Impacting Formulation Performance. Pharm Res. 2020;37:192. https://doi.org/10.1007/s11095-020-02909-6.
11. Zhao G, Wei K, Nguyen D, Lim HL, Rage B, Lu D. FDA Perspective on Dissolution Testing for Development of High-Risk Oral Drug Products Containing Amorphous Solid Dispersions (T1230–09–051). American Association of Pharmaceutical Scientist (AAPS) PharmSci 360 Meeting - Salt Lake City - October 22, 2024. Available from: https://posters.aaps.org/aaps/?menu=16&browseby=3&sortby=2&ce_id=2692&trend=19504#!*menu=16*browseby=3*sortby=2*ce_id=2692*trend=19504. Accessed 1 Nov 2024.
12. Extended-Release Oral Dosage Forms: Development, Evaluation, and Application of In Vitro/In Vivo Correlations - Guidance for Industry. U.S. Food and Drug Administration; 1997. Available from: https://www.fda.gov/regulatory-information/search-fda-guidance-documents/extended-release-oral-dosage-forms-development-evaluation-and-application-vitroin-in-vivo-correlations. Accessed 1 Nov 2024.
13. Suarez-Sharp S, Li M, Duan J, Shah H, Seo P. Regulatory Experience with In Vivo In Vitro Correlations (IVIVC) in New Drug Applications. AAPS J. 2016;18:1379–90. https://doi.org/10.1208/s12248-016-9966-2.
14. Kesisoglou F, Hermans A, Neu C, Yee KL, Palcza J, Miller J. Development of In Vitro–In Vivo Correlation for Amorphous Solid Dispersion Immediate-Release Suvorexant Tablets and Application to Clinically Relevant Dissolution Specifications and In-Process Controls. Journal of Pharmaceutical Sciences. 2015;104:2913–22. Available from: https://linkinghub.elsevier.com/retrieve/pii/S0022354916300715.
15. Honório TDS, Pinto EC, Rocha HVA, Esteves VSD, Dos Santos TC, Castro HCR, et al. In Vitro–In Vivo Correlation of Efavirenz Tablets Using GastroPlus®. AAPS PharmSciTech. 2013;14:1244–54. https://doi.org/10.1208/s12249-013-0016-4.
16 Abuhelwa AY, Mudge S, Hayes D, Upton RN, Foster DJR. Population In Vitro-In Vivo Correlation Model Linking Gastrointestinal Transit Time, pH, and Pharmacokinetics: Itraconazole as a Model Drug. Pharm Res. 2016;33:1782–94. https://doi.org/10.1007/s11095-016-1917-1.
17 Abuhelwa AY, Mudge S, Upton RN, Foster DJR. Population in vitro–in vivo pharmacokinetic model of first-pass metabolism: itraconazole and hydroxy-itraconazole. J Pharmacokinet Pharmacodyn. 2018;45:181–97. https://doi.org/10.1007/s10928-017-9555-8.
18. Veng-Pedersen P, Gobburu JVS, Meyer MC, Straughn AB. Carbamazepine level-A in vivo-in vitro correlation (IVIVC): a scaled convolution based predictive approach. Biopharm Drug Dispo. 2000;21:1–6. https://doi.org/10.1002/1099-081X(200001)21:1<1::AID-BDD207>3.0.CO;2-D
19. Zhang G, Sun M, Jiang S, Wang L, Tan Y, Wang L, et al. Investigating a Modified Apparatus to Discriminate the Dissolution Capacity In Vitro and Establish an IVIVC of Mycophenolate Mofetil Tablets in the Fed State. J Pharm Sci. 2021;110:1240–7. Available from: https://linkinghub.elsevier.com/retrieve/pii/S0022354920306201. Accessed 1 Nov 2024.
20. Ostrowski M, Wilkowska E, Bączek T. In vivo–in vitro correlation for amoxicillin trihydrate 1000 mg dispersible tablet. Drug Development and Industrial Pharmacy. 2009;25;35:981–5. Available from: http://www.tandfonline.com/doi/full/https://doi.org/10.1080/03639040902737492
21. Saibi Y, Sato H, Tachiki H. Developing In Vitro–In Vivo Correlation of Risperidone Immediate Release Tablet. AAPS PharmSciTech. 2012;13:890–5. https://doi.org/10.1208/s12249-012-9814-3.
22. Ruiz Picazo A, Martinez-Martinez MT, Colón-Useche S, Iriarte R, Sánchez-Dengra B, González-Álvarez M, et al. In Vitro Dissolution as a Tool for Formulation Selection: Telmisartan Two-Step IVIVC. Mol Pharmaceutics. 2018;15:2307–15. https://doi.org/10.1021/acs.molpharmaceut.8b00153.
23. Cámara-Martinez I, Blechar JA, Ruiz-Picazo A, Garcia-Arieta A, Calandria C, Merino-Sanjuan V, et al. Level A IVIVC for immediate release tablets confirms in vivo predictive dissolution testing for ibuprofen. International Journal of Pharmaceutics. 2022;614:121415. Available from: https://linkinghub.elsevier.com/retrieve/pii/S0378517321012217. Accessed 1 Nov 2024.
24. Kuemmel C, Yang Y, Zhang X, Florian J, Zhu H, Tegenge M, et al. Consideration of a Credibility Assessment Framework in Model-Informed Drug Development: Potential Application to Physiologically-Based Pharmacokinetic Modeling and Simulation. CPT Pharmacom & Syst Pharma. 2020;9:21–8. Available from: https://ascpt.onlinelibrary.wiley.com/doi/https://doi.org/10.1002/psp4.12479.
25. Assessing the Credibility of Computational Modeling and Simulation in Medical Device Submissions - Guidance for Industry and Food and Drug Administration Staff. U.S. Food and Drug Administration; 2023. Available from: https://www.fda.gov/regulatory-information/search-fda-guidance-documents/assessing-credibility-computational-modeling-and-simulation-medical-device-submissions. Accessed 1 Nov 2024.
26. Heimbach T, MusuambaTshinanu F, Raines K, Borges L, Kijima S, Malamatari M, et al. PBBM Considerations for Base Models, Model Validation, and Application Steps: Workshop Summary Report. Mol Pharmaceutics. 2024;21:5353–72. https://doi.org/10.1021/acs.molpharmaceut.4c00758.
27. Krug SA, Coutinho AL, Polli JE, Kane MA. Validation of a method for itraconazole and major metabolite hydroxyitraconazole for LC-MS/MS analysis with application in a formulation clinical study. J Pharm Biomed Anal. 2023;234:115505. Available from: https://linkinghub.elsevier.com/retrieve/pii/S0731708523002741. Accessed 1 Nov 2024.
28. Polli JE, Rekhi GS, Augsburger LL, Shah VP. Methods to Compare Dissolution Profiles and a Rationale for Wide Dissolution Specifications for Metoprolol Tartrate tablets. Journal of Pharmaceutical Sciences. 1997;86:690–700. Available from: http://linkinghub.elsevier.com/retrieve/pii/S0022354915503274. Accessed 1 Nov 2024.
29. Polli JE. A Simple One-Parameter Percent Dissolved Versus Time Dissolution Equation that Accommodates Sink and Non-sink Conditions via Drug Solubility and Dissolution Volume. AAPS J. 2022;25:1. https://doi.org/10.1208/s12248-022-00765-3.
30. The Use of Physiologically Based Pharmacokinetic Analyses — Biopharmaceutics Applications for Oral Drug Product

Development, Manufacturing Changes, and Controls (Guidance for Industry). 2020. Available from: https://www.fda.gov/regulatory-information/search-fda-guidance-documents/use-physiologically-based-pharmacokinetic-analyses-biopharmaceutics-applications-oral-drug-product. Accessed 1 Nov 2024.
31. Heykants J, Van Peer A, Van De Velde V, Van Rooy P, Meuldermans W, Lavrijsen K, et al. The Clinical Pharmacokinetics of Itraconazole: An Overview. Mycoses. 1989;32:67–87. Available from: https://onlinelibrary.wiley.com/doi/https://doi.org/10.1111/j.1439-0507.1989.tb02296.x.
32 Polli JE, Ginski MJ. Human drug absorption kinetics and comparison to Caco-2 monolayer permeabilities. Pharmaceutical Research. 1998;15:47–52. https://doi.org/10.1023/A:1011992518592.
33. Adhikari A, Seo PR, Polli JE. Characterization of Dissolution-Permeation System using Hollow Fiber Membrane Module and Utility to Predict in Vivo Drug Permeation Across BCS Classes. Journal of Pharmaceutical Sciences. 2022;111:3075–87. Available from: https://linkinghub.elsevier.com/retrieve/pii/S0022354922002957. Accessed 1 Nov 2024.
34. Itraconazole Capsule Dissolution Monograph. United States Pharmacopeia; 2019. Available from: https://www.uspnf.com/sites/default/files/usp_pdf/EN/USPNF/revisions/itraconazole-caps-rb-notice-20190531.pdf. Accessed 1 Nov 2024.
35. Herting M, Kleinebudde P. Studies on the reduction of tensile strength of tablets after roll compaction/dry granulation. European Journal of Pharmaceutics and Biopharmaceutics. 2008;70:372–9. Available from: https://linkinghub.elsevier.com/retrieve/pii/S0939641108001446.
36 Stewart AM, Grass ME. Practical Approach to Modeling the Impact of Amorphous Drug Nanoparticles on the Oral Absorption of Poorly Soluble Drugs. Mol Pharmaceutics. 2020;17:180–9. https://doi.org/10.1021/acs.molpharmaceut.9b00889.
37. Shah DD, Taylor LS. Chemistry and Ionization of HPMCAS Influences the Dissolution and Solution-Mediated Crystallization of Posaconazole Amorphous Solid Dispersions. Journal of Pharmaceutical Sciences. 2024;S0022354924003514. Available from: https://linkinghub.elsevier.com/retrieve/pii/S0022354924003514. Accessed 1 Nov 2024.
38. Men S, Polli JE. Microscope-enabled disc dissolution system: Concordance between drug and polymer dissolution from an amorphous solid dispersion disc and visual disc degradation. Journal of Pharmaceutical Sciences. 2024;S0022354924004854. Available from: https://linkinghub.elsevier.com/retrieve/pii/S0022354924004854.
39 Raines K, Agarwal P, Augustijns P, Alayoubi A, Attia L, Bauer-Brandl A, et al. Drug Dissolution in Oral Drug Absorption: Workshop Report. AAPS J. 2023;25:103. https://doi.org/10.1208/s12248-023-00865-8.
40. Westergaard H, Dietschy JM. The mechanism whereby bile acid micelles increase the rate of fatty acid and cholesterol uptake into the intestinal mucosal cell. J Clin Invest. 1976;58:97–108. Available from: http://www.jci.org/articles/view/108465.
41. Sugano K. Possible reduction of effective thickness of intestinal unstirred water layer by particle drifting effect. Int J Pharm. 2010;387:103–9. Available from: https://linkinghub.elsevier.com/retrieve/pii/S0378517309008710. Accessed 1 Nov 2024.
42. Patel RP, Taylor LS, Polli JE. Impact of drug incorporation into micelle on reduced griseofulvin and meloxicam permeation across a hollow fiber membrane. J Pharm Sci. 2024;S0022354924004520. Available from: https://linkinghub.elsevier.com/retrieve/pii/S0022354924004520.
43. Buchwald P. Direct, differential-equation-based in-vitro–in-vivo correlation (IVIVC) method. J Pharm Pharmacol. 2010;55:495–504. Available from: https://academic.oup.com/jpp/article/55/4/495/6148198.
44 Brockmeier D, Dengler HJ, Voegele D. In vitro ? In vivo correlation of dissolution, a time scaling problem? Transformation of in vitro results to the in vivo situation, using theophylline as a practical example. Eur J Clin Pharmacol. 1985;28:291–300. https://doi.org/10.1007/BF00543326.
45. Bapat P, Schwabe R, Paul S, Tseng Y-C, Bergman C, Taylor LS. Exploring biorelevant conditions and release profiles of ritonavir from HPMCAS-based amorphous solid dispersions. J Pharm Sci. 2024;S0022354924003162. Available from: https://linkinghub.elsevier.com/retrieve/pii/S0022354924003162.
46 Jantratid E, Janssen N, Reppas C, Dressman JB. Dissolution Media Simulating Conditions in the Proximal Human Gastrointestinal Tract: An Update. Pharm Res. 2008;25:1663–76. https://doi.org/10.1007/s11095-008-9569-4.
47. Kamba M, Seta Y, Kusai A, Nishimura K. Comparison of the mechanical destructive force in the small intestine of dog and human. International Journal of Pharmaceutics. 2002;237:139–49. Available from: https://linkinghub.elsevier.com/retrieve/pii/S0378517302000431.
48 Vardakou M, Mercuri A, Barker SA, Craig DQM, Faulks RM, Wickham MSJ. Achieving Antral Grinding Forces in Biorelevant In Vitro Models: Comparing the USP Dissolution Apparatus II and the Dynamic Gastric Model with Human In Vivo Data. AAPS PharmSciTech. 2011;12:620–6. https://doi.org/10.1208/s12249-011-9616-z.
49 Shameem M, Katori N, Aoyagi N, Kojima S. Oral Solid Controlled Release Dosage Forms: Roles of GI-Mechanical Destructive Forces and Colonic Release in Drug Absorption Under Fasted and Fed Conditions in Humans. Pharm Res. 1995;12:1049–54. https://doi.org/10.1023/A:1016270701021.
50. Garbacz G, Klein S, Weitschies W. A biorelevant dissolution stress test device – background and experiences. Expert Opin Drug Deliv. 2010;7:1251–61. Available from: http://www.tandfonline.com/doi/full/https://doi.org/10.1517/17425247.2010.527943.
51. Higuchi M, Yoshihashi Y, Tarada K, Sugano K. Minimum rotation speed to prevent coning phenomena in compendium paddle dissolution apparatus. Eur J Pharm Sci. 2014;65:74–8. Available from: https://linkinghub.elsevier.com/retrieve/pii/S0928098714003510. Accessed 1 Nov 2024.
52. Vaithianathan S, Raman S, Jiang W, Ting TY, Kane MA, Polli JE. Biopharmaceutic Risk Assessment of Brand and Generic Lamotrigine Tablets. Mol Pharmaceutics. 2015;12:2436–43. https://doi.org/10.1021/acs.molpharmaceut.5b00154.
53. Ting TY, Jiang W, Lionberger R, Wong J, Jones JW, Kane MA, et al. Generic lamotrigine versus brand-name LAMICTAL bioequivalence in patients with epilepsy: A field test of the FDA bioequivalence standard. Epilepsia. 2015;56:1415–24. Available from: https://onlinelibrary.wiley.com/10.1111/epi.13095. Accessed 1 Nov 2024.
54. Wagner JG. Pharmacokinetics for the Pharmaceutical Scientist. 1st ed. CRC Press; 2018. Available from: https://www.taylorfrancis.com/books/9781351425124.
55 Cao Y, Jusko WJ. Applications of minimal physiologically-based pharmacokinetic models. J Pharmacokinet Pharmacodyn. 2012;39:711–23. https://doi.org/10.1007/s10928-012-9280-2.
56. Brouwers J, Geboers S, Mols R, Tack J, Augustijns P. Gastrointestinal behavior of itraconazole in humans – Part 1: Supersaturation from a solid dispersion and a cyclodextrin-based solution. Int J Pharm. 2017;525:211–7. Available from: https://linkinghub.elsevier.com/retrieve/pii/S0378517317303198. Accessed 1 Nov 2024.